JOURNAL OF MATERIALS SCIENCE 18 (1983) 2437–2452

High resolution X-ray diffraction of fully and partially magnesium stabilized beta''-alumina ceramics

F. HARBACH
Brown, Boveri and Cie AG, Zentrales Forschungslabor, Eppelheimer Strasse 82, 6900 Heidelberg 1, Federal Republic of Germany

The dependence of the unit cell size of β''-Al_2O_3 on its sodium and magnesium content has been stated in the past in a contradictory manner. This situation is clarified on the basis of high resolution Guinier photographs of the X-ray diffraction of fully stabilized ternary β''-Al_2O_3 ceramics with compositions of $Na_{1+z}Mg_zAl_{11-z}O_{17}$. The lattice constant a_0 increases with increasing z over the range of 0.5 to 0.8. In contrast, the height H of the conduction slab decreases with increasing z. Both values level off at $z \geqslant 0.8$. This behaviour is discussed using simple models. The X-ray diffraction patterns of β''-Al_2O_3 ceramics can show considerable splittings of reflections with high Miller indices l for compositions which do not correspond to the above formula. These splittings can be attributed to the simultaneous presence of two different β''-Al_2O_3 component phases – a fully and a partially magnesium stabilized one. The excess sodium of the partially stabilized component phase is shown to be charge compensated by interstitial oxygen ions in the conduction slab, which is equivalent to the widely accepted compensation mechanism for the excess sodium of binary β-Al_2O_3.

1. Introduction

The Na/S secondary battery currently being tested by Brown Boveri and other companies offers the advantages of high power density and good electrical efficiency. The excellent ionic conductivity of the solid electrolyte ceramics that separate the reacting components (sodium and sulphur) inside a single cell is essential in order to obtain these advantages. The only solid electrolytes seriously considered for this purpose today are the sodium polyaluminates. Of these, sodium ions only exhibit outstanding conductivities in β- and β''-Al_2O_3 phases [1–4]. Single crystals of the β''-Al_2O_3 phase have even shown conductivities that, at 300° C, are five times higher than those of the β-Al_2O_3 phase ($1.06\ \Omega^{-1}\,cm^{-1}$ [5] compared to $0.21\ \Omega^{-1}\,cm^{-1}$ [6]).

This paper is part of an investigation that aims to clarify the structural constraints that have to be observed in the course of compositional and phase content changes in sodium polyaluminate solid electrolyte ceramics. It is concerned firstly with the composition dependence of the unit cell size of non-stoichiometric β''-Al_2O_3. In the literature, the dependence of the lattice constant a_0 on the β''-Al_2O_3 composition has not been discussed in depth and the conclusions drawn concerning the dependence of the lattice constant c_0 on the composition are contradictory.

Agreement has been found regarding the corresponding dependence for β-Al_2O_3. According to Dell and Moseley [6], the lattice constant c_0 of β-Al_2O_3 single crystals decreases with increasing sodium contents. c_0 drops from 2.255 to 2.235 nm between 5.0 mass % Na_2O (ca. $Na_2O{\cdot}11\ Al_2O_3$) and 7.7 mass % Na_2O (ca. $Na_2O{\cdot}7\ Al_2O_3$). Boilot *et al.* [7] find the same type of dependence of c_0 upon the sodium content, although they used magnesium doping to obtain higher sodium concentrations. Without the addition of magnesium, i.e. at $Na_2O{\cdot}11\ Al_2O_3$, they find $c_0 = 2.257$ nm in good accordance with Dell and Moseley.

Returning to β''-Al_2O_3, Boilot *et al.* [7] state

0022–2461/83 $03.00 + .12

that c_0 increases with increasing sodium content, whereas May and Henderson [8] ascertain that a diminishing sodium concentration leads to an expansion of the unit cell of β''-Al_2O_3 parallel to the c-axis.

The present paper seeks to clarify this point. Of course, it would be most desirable to use a variety of single crystals for a systematic investigation of the dependence of the size of the unit cell of β''-Al_2O_3 on its composition. For practical reasons – the ultimate goal is to produce solid electrolyte ceramics for the Na/S cell – attempts were made to prepare single phase β''-Al_2O_3 ceramics of different compositions.

A second topic of the present paper is the verification of the charge compensation mechanism in non-stoichiometric β''-Al_2O_3. This question has not received as much attention as it has for β-Al_2O_3.

2. Competitive structure models

2.1. Stoichiometric binary and ternary β''-Al_2O_3

In order to have a basis for the following discussion, the structures of the stoichiometric sodium polyaluminates β-Al_2O_3, binary β''-Al_2O_3 and ternary β''-Al_2O_3 are presented side by side in Fig. 1. ("Stoichiometric" and "non-stoichiometric" are used in the sense given by Boilot *et al.* [9, 10].) The figure is only explained in brief; more extensive presentations of the different structures may be found in the quoted literature.

The theoretical composition of β-Al_2O_3 is $Na_2O \cdot 11Al_2O_3$ [11]. It is often named two-block beta, because the unit cell consists of two "spinel blocks" that are separated by the conduction plane. In Fig. 1a, every spinel block is sketched by four lines that stand for the four cubic close-packed oxygen layers, of which a spinel block is

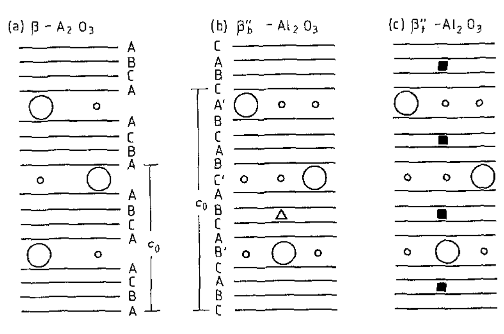

Figure 1 Schematic structure of stoichiometric β-Al_2O_3, binary and ternary β''-Al_2O_3.

composed. The sequence of these layers is indicated by capital letters (A, B, C). Aluminium ions occupy tetrahedral and octahedral sites in the oxygen frame. The conduction plane contains a mobile sodium ion (small open circle) and a spacer oxygen ion (large open circle). The space group of β-Al_2O_3 is $P6_3$/mmc.

β''-Al_2O_3 differs from β-Al_2O_3 by its symmetry, the structure is rhombohedral (space group $R\bar{3}$m). Three spinel blocks belong to the triply-primitive hexagonal cell and therefore, β''-Al_2O_3 is often named three-block beta. The sequence of the oxygen layers is consistently face-centred cubic and it even includes the oxygen ion of the interlayer. The spacer oxygen of the β''-Al_2O_3 structure can be regarded, therefore, as a remainder of an oxygen layer belonging to an overall face-centred cubic structure. In Fig. 1, the interlayers of β''-Al_2O_3 have been labelled with primed capital letters.

The construction of the β''-Al_2O_3 lattice results in a doubling of the number of energetically favoured sodium sites. Furthermore, the interlayers that contain these sodium ions are not two-dimensional conduction planes, but show a slight modulation of the distribution of the sodium ions in the c-direction and therefore are better named conduction slabs. The exact composition of β''-Al_2O_3 depends on how many additional sodium ions are actually present and on how their additional charge is balanced.

According to Yamaguchi and Suzuki [1], the stoichiometric β''-Al_2O_3 phase has a composition $Na_2O \cdot 5Al_2O_3$ or more correctly [6, 12] $Na_2O \cdot$ 5 1/3 Al_2O_3. The additional positive sodium ion per unit cell is charge balanced by a third aluminium vacancy. In Fig. 1b, one vacancy (open triangle) has been attributed to the intermediate spinel block of the hexagonal cell instead of a third aluminium vacancy to each spinel block.

An alternative to charge compensation by vacancies would be to replace a trivalent aluminium ion of a spinel block by a divalent ion for each additional sodium ion included in the β''-Al_2O_3 structure. In order to distinguish the above model of the β''-Al_2O_3 structure from the modified one, the former will be called stoichiometric binary β''-Al_2O_3 and the latter stoichiometric (fully stabilized) ternary β''-Al_2O_3. If a magnesium ion is chosen as a divalent ion, the composition of the stoichiometric ternary β''-Al_2O_3 phase is $Na_2O \cdot MgO \cdot 5\,Al_2O_3$ or $Na_2MgAl_{10}O_{17}$ [2]. The magnesium ion (filled square) preferentially substitutes for

one of the aluminium ions in tetrahedral coordination in the middle of a spinel block of ternary β''-Al_2O_3 [13, 14].

2.2. Non-stoichiometric β''-Al_2O_3

All hitherto discussed stoichiometric compositions can only be synthesized using special preparation techniques [9, 15–17]. β-Al_2O_3 ceramics and single crystals are generally found to contain excess sodium, whereas standard β''-Al_2O_3 is sodium deficient compared with the respective idealized formulae.

For (binary) β-Al_2O_3, Roth *et al.* [14] proved that excess sodium is charge-balanced by the insertion of oxygen ions on interstitial sites of the conduction plane. The aluminium–vacancy model, which had been proposed earlier by Peters *et al.* [18] for β-Al_2O_3 and which corresponds to the Yamaguchi–Suzuki structure model for binary β''-Al_2O_3 [1, 6], could not be confirmed. The aluminium vacancies that are connected with interstitial oxygen ions belong to Frenkel defects, which "mechanically" stabilize these additional oxygen ions and do not lead to an alteration of the charge of the spinel blocks adjacent to an excess sodium ion.

Up to now, a model does not exist for the sodium deficiency of β''-Al_2O_3 which is as commonly accepted as the Roth model for β-Al_2O_3.

For fully stabilized ternary β''-Al_2O_3, Bettman and Peters [2] expect that a reduction of the sodium content can just be compensated for by a reduction in the magnesium content according to the following formula:

$$Na_{1+z}Mg_zAl_{11-z}O_{17}, \qquad 0 < z < 1. \quad (1)$$

Most single crystals of β''-Al_2O_3 that have been grown up to now [5, 7, 14, 19–21] have been specified as having compositions corresponding to Formula 1 with z around 2/3. Collin *et al.* [22] have deduced a superstructure model for this value from X-ray scattering experiments. The original Bettman–Peters composition $Na_2O \cdot MgO \cdot 5Al_2O_3$ follows from Formula 1 for $z = 1$. If we take this composition for the stoichiometric limit of the ternary β''-Al_2O_3 composition range, then z can be regarded as a stoichiometry parameter or as a measure of the degree of stoichiometry of a given fully magnesium stabilized β''-Al_2O_3 phase.

A preliminary, more comprehensive model for the charge balancing of a varying number of sodium ions in the conduction slab of β''-Al_2O_3 cannot only consist of the Bettman–Peters conception. It has to be conceived in such a way to cover the Yamaguchi–Suzuki model of aluminium vacancies in the spinel block and to provide for the possibility of interstitial oxygen ions in the conduction slab as well. The latter would correspond to the Roth model for β-Al_2O_3. A composition that takes all three conceptions into consideration can be expressed by the following formula:

$$Na_{1+3x+2y+z}Mg_zAl_{11-x-z}O_{17+y}(Al_x)\,(O_y)_i. \quad (2)$$

$Na_{3x+2y+z}$ stands for the additional sodium that is in excess of the content of the stoichiometric β-Al_2O_3 structure and whose charge has to be compensated for suitably by the incorporation of magnesium Mg_z or other divalent ions, interstitial oxygen $(O_y)_i$ or aluminium vacancies (Al_x). The latter two are contained in Formula 2 in a redundant form. The following expression

$$[Na_{1+3x+2y+z}O_{1+y}(O_y)_i]\,[Mg_zAl_{11-x-z}O_{16}(Al_x)] \quad (3)$$

stresses the possible partition of ions between the conduction slab (first part) and the spinel block (second part).

A further extension of Formulae 2 and 3 to cover charge compensation by univalent ions as well would be straight forward and need not be included here.

3. Experimental procedure

3.1. X-ray diffraction

The present investigation is confined to the X-ray diffraction of sodium polyaluminate ceramics at room temperature. The experimental assembly consists of a Siemens X-ray generator, which includes a 750 W copper X-ray tube (operated at 600 W) with vertical line focus, and a Huber Guinier system comprising a focusing Precision Monochromator (Johansson type Germanium crystal plate) for Cu$K\alpha_1$ radiation, Soller slits and a Guinier Powder Chamber operating on the basis of Seemann–Bohlin focusing. The photographs are taken in asymmetric transmission. Partition panes for recording a maximum of 5 specimens are available, although only 3 specimens are routinely investigated in parallel. One of the two outermost sections is used for the silicon reference powder. All samples are exposed for 8 h. The Guinier technique together with the use of a monochromator

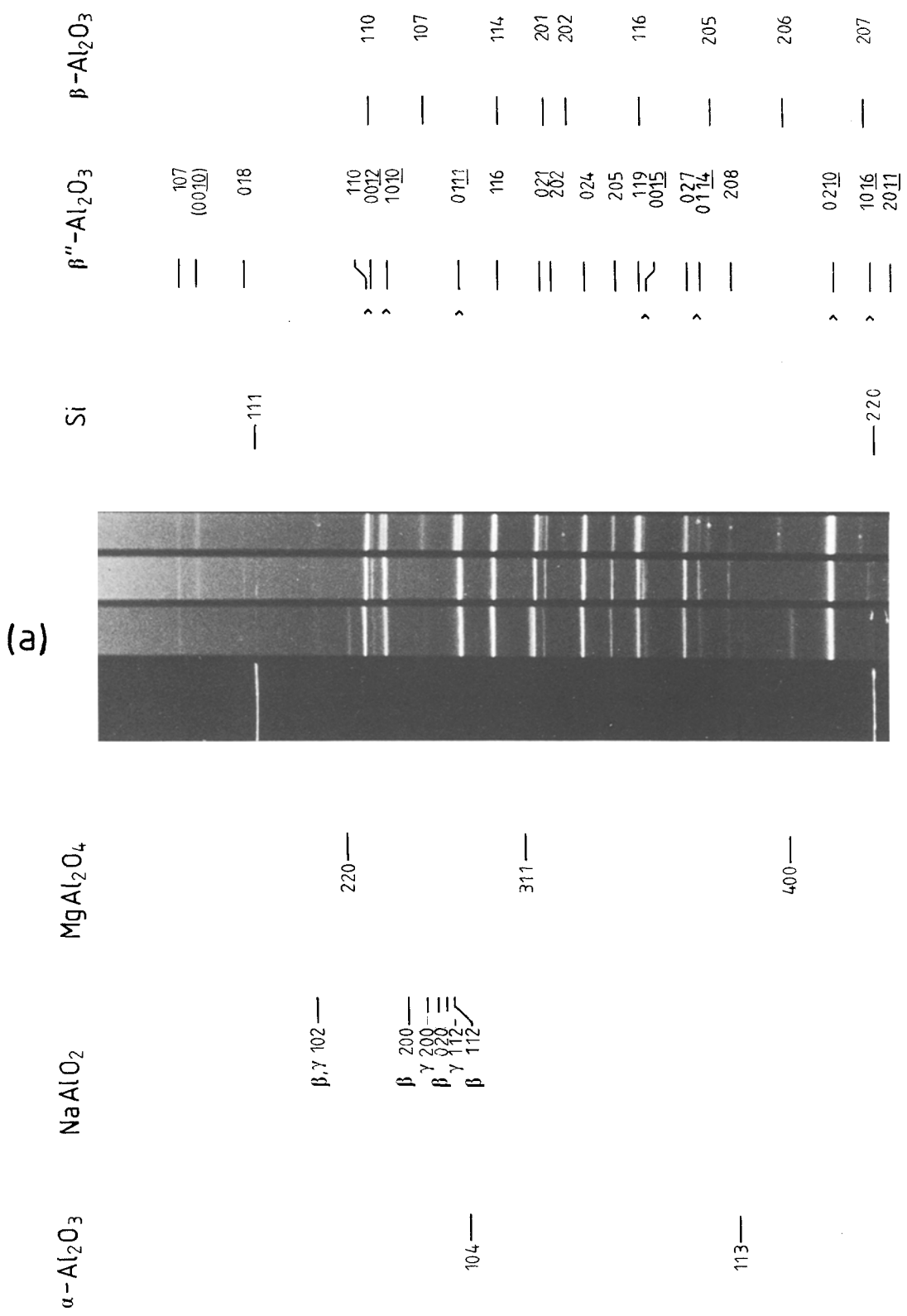

Figure 2 Quadruple Guinier photograph of three sodium polyaluminates with different compositions (samples 1, 4 and 6) and silicon reference (from above). (a) shows the angular range $25° \leqslant 2\theta \leqslant 48°$ and (b) shows the angular range $47° \leqslant 2\theta \leqslant 71°$.

Figure 2 Continued.

and special focusing methods guarantees a resolution that is far higher than can be achieved using standard powder diffractometers [12]. The choice of single-coated film (Kodak) retains most of the resolving power of the camera.

3.2. Ceramic samples

The ceramic samples are prepared using standard powder preparation methods, isostatic pressing at 200 MPa and sintering between 1590 and 1670° C in air. The compositional variation has some influence on the choice of the optimal preparation method, the sinterability and final quality of the different solid electrolyte ceramics. This is not discussed further.

The ceramic samples investigated were ground in a vibratory ball mill, annealed at 800° C for 2 h, cooled and stored under flowing dry nitrogen. The Guinier photographs were taken as soon as possible after annealing the powders. Thus, atmospheric influences on peak positions and peak widths were almost completely excluded [23].

Six ceramic samples together with their X-ray diffraction patterns are treated here in a more comprehensive manner. These are

1. 8.56 mass % Na_2O; 2.23 mass % MgO; balance Al_2O_3. This composition is 50% magnesium deficient compared with Formula 1. It results from Formulae 2 and 3 for $z = 3x = 1/3$ and is a special case of the class of compositions where $z = 1/3$ and $3x + 2y = 1/3$. These are all close to the Brown Boveri standard composition for solid electrolyte ceramics used as separators in Na/S cells i.e. 8.70% Na_2O; 2.25% MgO; balance Al_2O_3.

2. 8.55 mass % Na_2O; 3.34 mass % MgO; balance Al_2O_3. This composition with 25% magnesium deficiency has been calculated from Formulae 2 and 3 for $z = 1/2$ and $3x = 1/6$.

3. 8.54 mass % Na_2O; 4.00 mass % MgO; balance Al_2O_3. This composition with 10% magnesium deficiency has been calculated for $z = 0.60$ and $3x = 0.067$.

4. 8.53 mass % Na_2O; 4.44 mass % MgO; balance Al_2O_3. This is a fully stabilized ternary composition corresponding to Formula 1 with $z = 2/3$.

5. 8.52 mass % Na_2O; 4.52 mass % MgO; balance Al_2O_3. This composition contains 2% excess magnesium compared with sample 4.

6. 10.13 mass % Na_2O; 6.59 mass % MgO; balance Al_2O_3. This sample has been tested in the course of an investigation of stoichiometric ternary β''-Al_2O_3, i.e. with $z = 1$ [17].

The same starting powders and identical fabrication routes including sintering at 1630° C were used for the preparation of these six samples. The starting powders for samples 1 to 5 were mixed with Na_2O contents that were 5% (1.05 times) higher than the above values in order to compensate for Na_2O losses during preparation and sintering. Therefore the composition of sample 5 can equally well be classified as a fully magnesium stabilized one with $z = 0.68$ instead of $z = 2/3$ plus 2% excess magnesium. The procedure used with samples 1 to 5 was adopted for all other ceramics mentioned in this paper except for sample 6 where the above composition was used without further additions. The nominal Na_2O content and the Na_2O content of the fired product has only been checked for sample 1 using silver exchange in an $AgNO_3$ bath at 300° C. The measured value of (8.61 ± 0.02) mass % is in satisfactory agreement with the desired value of 8.56 mass %.

3.3. Phase content and lattice constant evaluation

The evaluation of lattice constants is confined normally to the measurement of the positions of a few representative peaks. In this case, each sample has to be checked to determine whether it can be regarded as single phase β''-Al_2O_3. This is due to the choice of the ceramic preparation route for each beta″-alumina. Principally, each visible peak is indexed and attributed to one of the phases β-, β''-Al_2O_3, β-, γ-$NaAlO_2$, spinel $MgAl_2O_4$ or corundum α-Al_2O_3. Other possible phases in the ternary sodium polyaluminate phase field such as β'''-, β''''-Al_2O_3, δ-$NaAlO_2$ need not be taken into account. Only samples that are single phase β''-Al_2O_3 with perhaps a weak $NaAlO_2$ content are considered without any reservations for further processing which involves the use of the least squares refinement program LATCON [24] to yield the lattice constants a_0 and c_0 and their standard deviations.

4. Results

The 2θ range from 25° to 71° of a quadruple Guinier photograph (positive) of samples 1, 4 and 6 and of the silicon reference powder is shown in Figs. 2a and b. The indexing of all visible reflections of the four Guinier photographs is included. The β-Al_2O_3, β''-Al_2O_3 and silicon reflections are given above the photographs, the reflections of the

unwanted phases $NaAlO_2$, spinel and corundum below.

The presence of β-Al_2O_3 is only visible with sample 1. A β-Al_2O_3 content of about 10% is typical for compositions in the vicinity of the Brown Boveri standard composition.

Sample 6 differs from samples 1 and 4 as it shows a significant spinel content. This spinel content is due to insufficient homogeneity of the relatively high magnesium content in the starting powder of the sample [17]. Sample 6 differs in a further point from samples 1 and 4. Their diffraction patterns contain a very weak, broad peak at $2\theta = 26.6°$, which is absent in the diffraction pattern of sample 6. The interplanar spacing that can be derived from the diffraction angle of 26.6° is 0.335 nm. This value corresponds quite well to $c_0/10$. Therefore, it should be indexed as $00\underline{10}$. A reflection of this type is forbidden according to the extinction rules for rhombohedral lattices although its appearance can nevertheless be caused by lattice imperfections. A "forbidden" peak as above is not present in sample 6 which shows that the composition of this sample agrees with the expected stoichiometric ternary composition. (The apparent spinel phase content, which should lead to a reduction in the magnesium content of the remaining β''-Al_2O_3 phase can be balanced by the corundum phase content, which is also present in sample 6.)

All three samples show a weak and diffuse $NaAlO_2$ 102 reflection. Since this reflection is neither the strongest β-$NaAlO_2$ reflection nor the strongest γ-$NaAlO_2$ reflection and since on the other hand it is the strongest $NaAlO_2$ reflection actually present, it must be a superposition of a β- and γ-$NaAlO_2$ 102 reflection, although γ-$NaAlO_2$ should be unstable at room temperature.

The three samples differ in their peak positions as well. The 110, 300 and 220 reflections show the most prominent shifts. They move to lower diffraction angles going from sample 1 to 6. These peaks only depend on the lattice constant a_0. Therefore it follows that a_0 increases from sample 1 to 4 to 6, i.e. in the same sense as the magnesium content of these samples increases.

Reflections with a relatively high Miller index l, whose positions are dominated by the influence of the lattice constant c_0, do not show a comparatively obvious compositional dependence. They seem to shift to higher diffraction angles moving from sample 4 to sample 6. (For example, $00\underline{12}$ and $20\underline{20}$; the refined c_0 values are 3.356 and 3.348 nm, respectively.) A significant splitting of these reflections for sample 1 forbids further conclusions to be drawn immediately. The respective splittings are marked by angles. Split peaks which partly coincide with other reflections have also been marked if recalculations of the positions of the component peaks yielded a significant and appropriate splitting (cf. Section 6).

Additional information on peak splittings can be obtained from Figs. 3a and b. The X-ray diffraction patterns of samples 2, 3 and 5 are displayed in these figures which include the indexing of all visible β''-Al_2O_3 peaks. Splittings of β''-Al_2O_3 are marked with angles as in Fig. 2.

Samples 2 and 3 (Fig. 3) show the same split diffraction peaks as sample 1 (Fig. 2). The intensities of the low angle (left hand side) component peaks increase with increasing magnesium content and the intensities of the high angle (right hand side) component peaks decrease with increasing magnesium content, i.e. from samples 1 to 3. At the same time, the low angle component peaks approach the high angle component peaks. Both effects can best be seen for lines $10\underline{10}$, $01\underline{11}$ and $20\underline{20}$.

Samples 4 and 5 that have about the same sodium contents as samples 1 to 3 do not show any splittings. Therefore, it can be stated that the splittings disappear if with a fixed sodium content, the magnesium content is increased in a manner such that the whole composition corresponds to the requirements of Formula 1. This in fact happens when going from sample 1 to samples 4/5. In the same way, sample 6 does not show splittings, since its composition corresponds to Formula 1 as well.

Lines indexed as $hk0$ are relatively narrow and move to lower diffraction angles going from sample 2 to 3 and to 5. It follows therefore, as shown for the samples of Fig. 2, that the lattice constant a_0 shows a tendency to increase with increasing magnesium content. (The refined values for all six samples are 0.5616, 0.5621, 0.5622, 0.5625, 0.5624 and 0.5628 nm, respectively. For the evaluation of the values for samples 1 to 3 cf. Section 6 and Table I.)

As shown above, the restriction to fully stabilized β''-Al_2O_3 phases leads to drastic simplifications of the X-ray diffraction patterns and allows a meaningful investigation of the dependence of the unit cell size of ternary β''-Al_2O_3 upon its

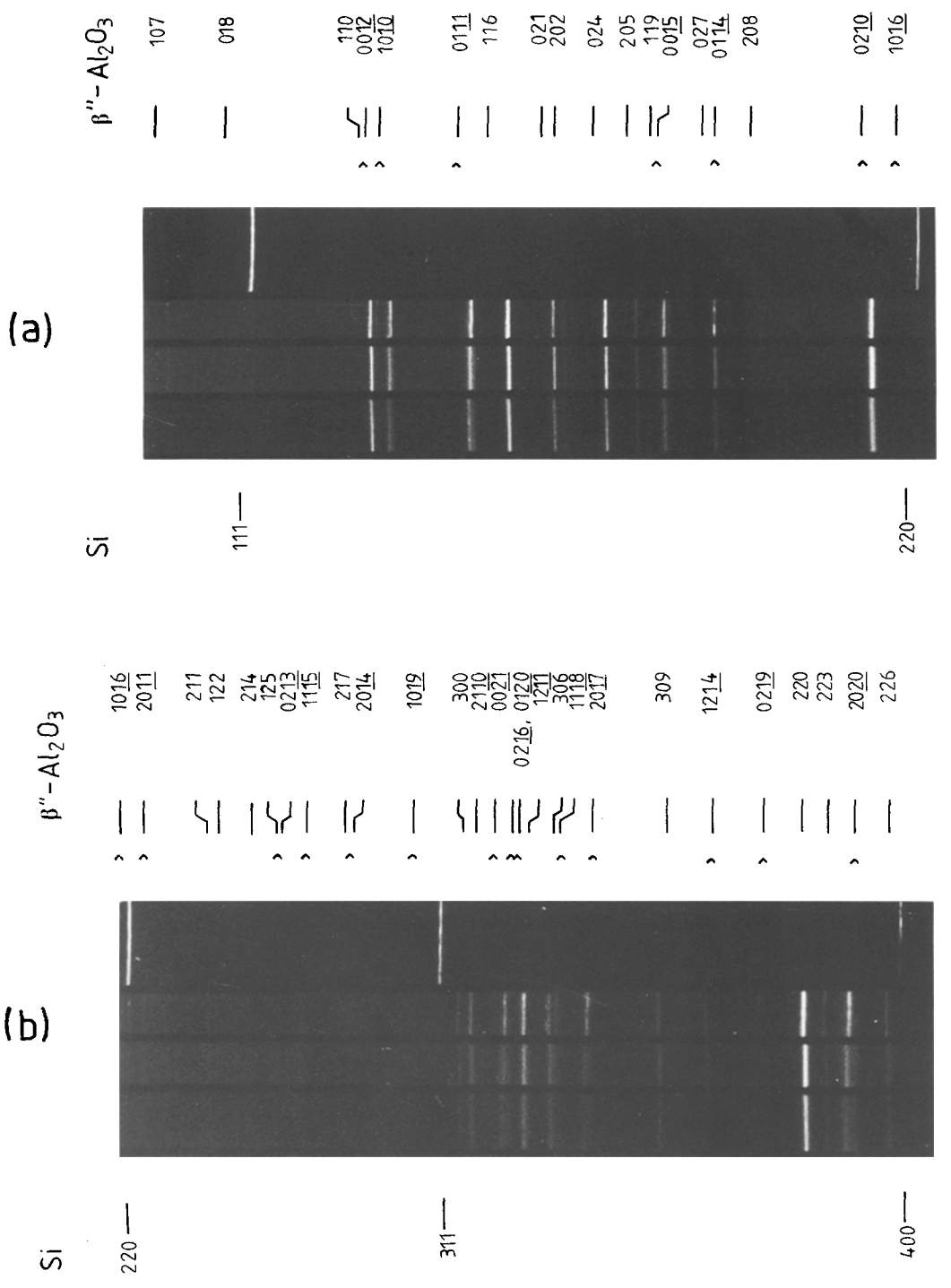

Figure 3 *Quadruple Guinier photograph of silicon reference and three beta-aluminas with different compositions (samples 5, 3 and 2, from above). (a) shows the angular range $25° \leqslant 2\theta \leqslant 48°$ and (b) the angular range $47° \leqslant 2\theta \leqslant 71°$.

*The intensities of the diffraction lines in Fig. 3 are somewhat lower than in Fig. 2; several very weak lines present in Fig. 2 are not detectable. This is due to the fact that the film material used for Fig. 2 (Kodak Film Radiographique, une face sans écran, 35 mm non perforé) is no longer manufactured. Kodak SB-392, CAT 161 8669, 35 mm × 7.5 m, had to be used instead.

TABLE I Results of the X-ray diffraction of ceramics with different compositions $Na_{1+3x+2y+z}Mg_zAl_{11-z-x}O_{17+y}$, but identical sodium contents $Na_{1.67}$. Sample 5 has been designed to a slightly higher sodium content $Na_{1.68}$.

Sample number	Sample designation	z	$3x + 2y$	Symbol	a_0 ± 0.0002 (nm)	c_0 ± 0.002 (nm)	H ± 0.0005 (nm)	Remarks
1	V63-C51c-57	0.33	0.33	[2] g	0.5616	3.373	0.2587	intensity ratio g:k ca. 1:1; $NaAlO_2$;
				k	0.5616	3.355	0.2527	10% β-Al_2O_3
2	V77-E05-77	0.50	0.17	[2] g	0.5620	3.368	0.2565	intensity ratio g:k ca. 2:1
				k	0.5622	3.350	0.2502	
3	V78-E05-77	0.60	0.067	[2] g	0.5621	3.365	0.2553	
				k	0.5623	3.349	0.2500	only weak k-reflections
4	V62-C51c-57	0.67	–	[2]	0.5625	3.356	0.2517	$NaAlO_2$
5	V79-E05-77	0.68	–	[2]	0.5624	3.356	0.2518	very sharp relections

sodium and magnesium content. Such an investigation is discussed in the next section. The peak splittings that occur for samples 1 through 3 are discussed in Section 6.

5. Fully stabilized ternary β''-Al_2O_3

5.1. Lattice constant changes with increasing stoichiometry

Diffraction patterns of a variety of β''-Al_2O_3 ceramics with compositions corresponding to Formula 1 have been investigated in addition to samples 4 to 6. The investigated composition range had to be restricted to values of z between 0.5 and 1. For $z < 0.5$, the ceramic production turned out to be of little practical use because of low densification, the unavoidable occurrence of a β-Al_2O_3 phase content and moderate ionic conductivity. For z approaching 1, severe problems with second phases developed [17].

The lattice constants a_0 and c_0 that could be deduced for the respective triply-primitive hexagonal unit cells are displayed in Figs. 4a and b, respectively. Those values that correspond to ceramic samples with a visible spinel content are only included as they give additional information that would otherwise not have been at hand. The respective symbols are given in parentheses. Identical symbols have been used for ceramics that may differ in composition, but have otherwise been subjected to the same preparation conditions (raw material, powder preparation, sintering route). The meanings of the different symbols shall not be discussed in this context for proprietary reasons. Numbers in open symbols refer to the maximal temperatures during sintering (1: 1590° C, 2: 1630° C, 3: 1650° C, 4: 1670° C); symbols without numbers always indicate a sintering temperature of 1620 to 1630° C.

Two things can be concluded from Figs. 4a and b. Firstly, the a_0 values scatter rather strongly; yet, a tendency towards an increase of a_0 with increasing z can be stated. Secondly, the c_0 values obviously decrease with increasing z; here, the scatter is considerable as well. Above $z \simeq 0.73$, a_0 as well as c_0 seem to level off.

If inspite of the disturbing scatter a linear dependence of a_0 and c_0 on z is assumed, at least for $z \leqslant 0.73$, then the following relations are obtained:

$$a_0(z)/\text{nm} = 0.5595 + 0.00406z \quad (4)$$

and

$$c_0(z)/\text{nm} = 3.417 - 0.0931z. \quad (5)$$

In the first case, the correlation coefficient $|r| = 0.65$ is hardly meaningful; in the second case, $|r| = 0.85$ is acceptable.

However, it has to be taken into account that the extension of the hexagonal cell of β''-Al_2O_3 in the direction of the c-axis is affected by a_0. If one assumes that a_0 is only defined by the size of one spinel block, the contribution of a spinel block to the lattice constant c_0 can be assessed in a straightforward manner due to the cubic close packing of the oxygen ions of the spinel block. It then follows that the height H of a single conduction slab or, more correctly, the thickness of the spacer oxygen of the conduction slab in the direction of the c-axis can be calculated by the following equation (see Appendix):

$$H = \frac{c_0}{3} - 1.5413a_0. \quad (6)$$

Fig. 5 clearly demonstrates that the scatter of

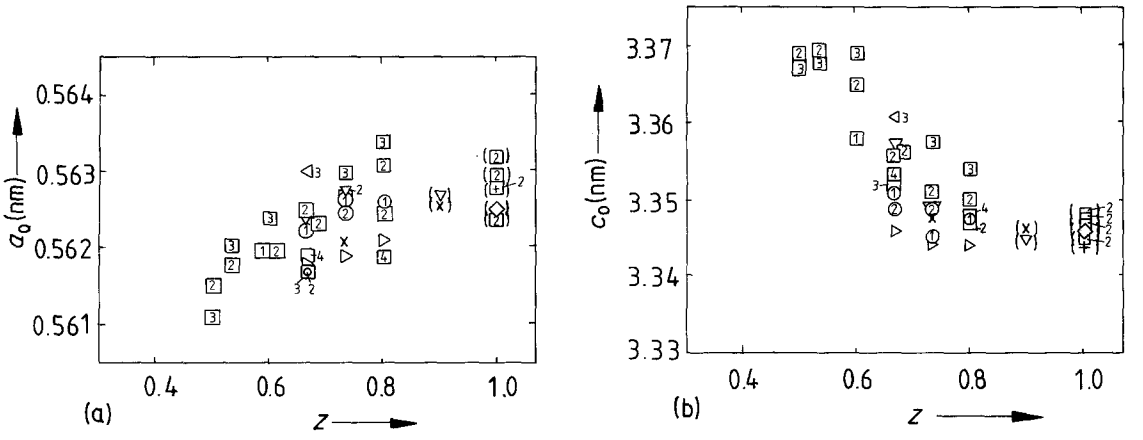

Figure 4 Dependence of the lattice constants (a) a_0 and (b) c_0 on the stoichiometry parameter z for ceramics with compositions $Na_{1+z}Mg_zAl_{11-z}O_{17}$.

the a_0-values is mainly responsible for the scatter of the c_0-values. After elimination of the contributions of the spinel blocks to the c_0-values, the scatter of the remaining thicknesses H of the conduction slabs of the different β''-Al_2O_3 compositions is largely reduced and shows a clear linear dependence of H upon the degree of stoichiometry of the beta''-aluminas, at least up to $z = 0.73$. Above $z = 0.73$, H levels off, in a similar manner to that found for a_0 and c_0.

The following linear relation is valid between $z = 0.50$ and 0.73:

$$H(z)/\text{nm} = 0.2761 - 0.03697z \qquad (7)$$

based on a correlation coefficient $|r| = 0.95$.

The above relations may additionally be

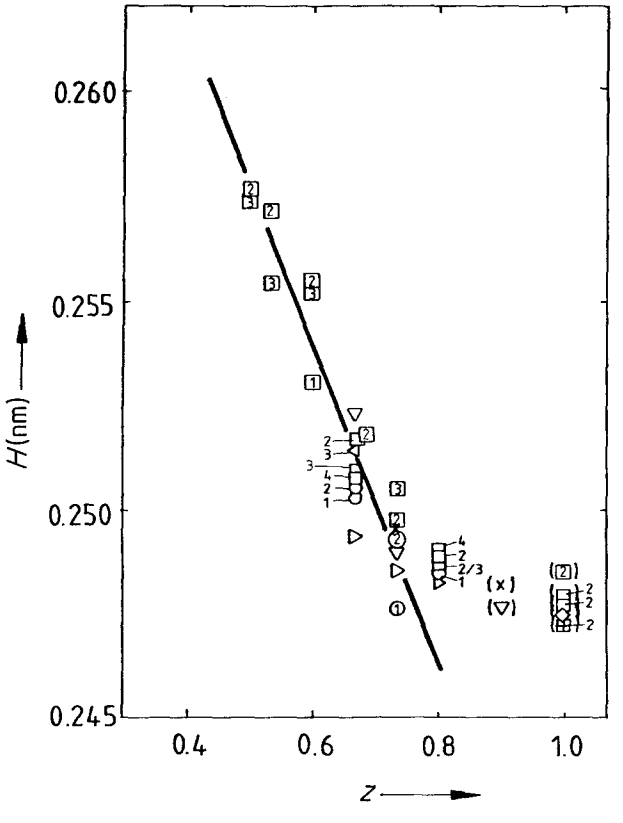

Figure 5 Height H of the conduction slab of ternary β''-Al_2O_3 ceramics as a function of their stoichiometry parameters z. The inserted line is the regression line for $0.50 \leqslant z \leqslant 0.73$.

checked against specifications of ternary Na^+-β''-Al_2O_3 single crystals that are given in the literature. Bettman and Peters [2] do not state a composition for the single crystal investigated. Their structural analysis yields the lattice constants $a_0 = 0.5614$ nm and $c_0 = 3.385$ nm. From Equation 7, a composition with $z = 0.35$ follows (which is below the range of validity of the equation). Brown *et al.* [21] specify their Oak Ridge single crystal as follows: z between 0.67 and 0.80, $a_0 = 0.56230$ nm and $c_0 = 3.3536$ nm. a_0 and c_0 inserted into Equations 4 through to 7 yields a composition of $z = 0.68 \pm 0.01$. Another Oak Ridge single crystal is reported to have a composition with z between 0.6 and 0.7 and lattice constants $a_0 = 0.5623$ nm and $c_0 = 3.3591$ nm [20]. From Equation 7, the composition should be 0.62. A single crystal with very similar unit cell dimensions has been described by Roth [25]: $a_0 = 0.5623$ nm, $c_0 = 3.360$ nm. The composition given as $z = 0.60$ is in good accordance with the value $z = 0.62$ that again follows from Equation 7.

In the following two subsections, the influence of magnesium doping and the influence of the sodium ion density upon the unit cell size of ternary β''-Al_2O_3 is discussed using simplified models. Let us first assume that doping of the spinel blocks by magnesium ions only affects a_0 and that H only depends upon the sodium concentration.

5.2. z-dependence of a_0

According to Roth *et al.* [13, 14], magnesium substitutes for aluminium on tetrahedral sites near the centre of a spinel block. A swelling of the spinel blocks due to incorporation of magnesium ions can be explained accordingly by the different sizes of the magnesium and aluminium ions, their ionic radii being

$$r_{Mg^{2+}} = 0.065\,\text{nm} \text{ and } r_{Al^{3+}} = 0.050\,\text{nm}. \quad (8)$$

γ-Al_2O_3 and spinel $MgAl_2O_4$ have structures that are quite similar to the structure of the spinel block of β''-Al_2O_3 [4]. γ-Al_2O_3 has all the tetrahedral sites occupied by aluminium ions inside the oxygen close packing. Spinel has only magnesium ions on these tetrahedral sites (4 tetrahedral sites per 16 oxygen ions). The latter constants a_0' of both (cubic) structures clearly reflect the different occupancies of the tetrahedral sites in accordance with Equation 8:

$$\begin{aligned} a_0'(MgAl_2O_4) &= 0.808\,\text{nm} \\ a_0'(\gamma\text{-}Al_2O_3) &= 0.790\,\text{nm}. \end{aligned} \quad (9)$$

According to Felsche [4], the lattice constants a_0' of these structures are related to the usual lattice constant a_0 of β''-Al_2O_3 by

$$a_0'(\beta''\text{-}Al_2O_3) = (2)^{1/2} a_0(\beta''\text{-}Al_2O_3). \quad (10)$$

A comparison of a highly magnesium doped β''-Al_2O_3 unit cell and the unit cell of spinel (corresponding to $z = 4$!) cannot be made. In Fig. 4a, a_0 seems to reach a constant value of about 0.563 nm as from $z = 0.8$. An extrapolation of Equation 4 to values above $z = 0.73$ is therefore excluded.

On the other hand, $a_0'(\beta''\text{-}Al_2O_3)$ can be extrapolated and recalculated from Equation 4 for $z = 0$, i.e. without a magnesium ion inside a spinel block, which results in:

$$a_0'(\beta''\text{-}Al_2O_3, z = 0) = (2)^{1/2} 0.5595\,\text{nm} = 0.791\,\text{nm}$$

which is in good agreement with the corresponding lattice constant of γ-Al_2O_3.

5.3. z-dependence of H

The extrapolation of Formula 1 to $z = 0$ yields the composition of a β''-Al_2O_3 structure that is equal to the composition $Na_2O \cdot 11\,Al_2O_3$ of stoichiometric β-Al_2O_3. In this case, the twofold negative charge of a spacer oxygen of the conduction slab is compensated by one positively charged sodium ion in the conduction slab and by the positive charge of a spinel block. Referred to a complete lattice, each spacer oxygen can be regarded as being surrounded by a symmetrical positive charge distribution. Its ionic radius should agree therefore with the Pauling radius of an oxygen ion $r_{O^{2-}} = 0.140$ nm [26]. Indeed, the extrapolation of $H(z)$, which represents the diameter of the spacer oxygen in the direction of the c-axis, to $z = 0$ yields $H(z = 0) = 0.2761$ nm, which is obviously not far from twice the Pauling radius.

As long as an increasing sodium concentration in the conduction slab is compensated by an increasing magnesium content in the adjacent spinel blocks, as given according to Formula 1, the positive charge of the conduction slab increases and the positive charge of the adjacent spinel blocks decreases. This must lead to a deformation of the negatively charged electronic cloud of the spacer oxygen, away from the spinel blocks and directed towards the neighbouring sodium ions in the conduction slab. The resulting reduction of the

extension of the spacer oxygen in the direction of the c-axis, i.e. the resulting reduction of $H(z)$ with increasing z is clearly displayed in Fig. 5.

Experience shows [26] that the diminuition of the diameter of an oxygen ion should have a limit near 0.25 nm. Fig. 5 in fact shows that H does not drop below 0.247 nm, even if z exceeds 0.8.

6. Partially stabilized ternary β''-Al_2O_3

Samples 1 to 3 are now used to explain the peak splittings and to clarify the charge compensation mechanism for ternary β''-Al_2O_3 ceramics where sodium contents are only partially stabilized by magnesium. Samples 4 and 5, which have about the same sodium content, serve as the fully stabilized reference specimens. The five samples are summarized in Table I for better reference during the following discussion.

Referring to the Brown Boveri standard composition with approximately 50% magnesium deficiency, Felsche [12] interpreted the splittings of some diffraction lines as being due to the presence of two β''-Al_2O_3 phases, a binary and a ternary one. The low angle component of a split peak is attributed to binary β''-Al_2O_3 $Na_2O{\cdot}5\ 1/3\ Al_2O_3$ (i.e. $z = y = 0; x = 1/3$ in Formulae 2 and 3) and the high angle portion to ternary β''-Al_2O_3 $Na_2O{\cdot}MgO{\cdot}5\ Al_2O_3$ (i.e. $z = 1, x = y = 0$). However, this model requires some modification. Firstly, it results in sodium and magnesium contents that are too high compared to the actual composition. As long as the principle concept ($z = 0$ for one component phase, $x = 0$ for the other and $y = 0$ for both) is retained, this model can be corrected by lowering x and z. Formula 2 is then reduced to

$$Na_{1+z+3x}Mg_zAl_{11-z-x}O_{17} \qquad (11a)$$

and can be split up to yield

$$\tfrac{1}{2}\cdot(Na_{1+6x}Al_{11-2x}(Al_{2x})O_{17} + Na_{1+2z}Mg_{2z}Al_{11-2z}O_{17}). \qquad (11b)$$

The first summand between the parentheses would be the binary component phase, the second one the ternary component phase.

With $z = 3x = 1/3$ (the composition of sample 1) both component phases differ in their spinel blocks, but not in their conduction slabs (cf. Formula 3). One would expect therefore that the most stringent splittings for sample 1 in Fig. 2 should be connected with $hk0$ lines, since only these are only connected with the lattice constant a_0, which itself is preferentially influenced by the spinel block structure. Exclusive splittings of $00l$ lines and of other peaks with a relatively high Miller index l should, however, be caused by differences in the conduction slabs, which are not provided by the Felsche model.

From this, one has to conclude that a new model has to be applied for the interpretation of the peak splittings. A charge compensation of excess sodium by oxygen interstitials is taken into account for β''-Al_2O_3, based on the findings of Roth *et al.* [14] and on the theoretical considerations of Wang [27] concerning the charge compensation mechanism in β-Al_2O_3.

The new model implies $x = 0$ and $y \neq 0$ in Formulae 2 or 3, at least as long as partially stabilized compositions are concerned. Formula 11, therefore, has to be changed to

$$Na_{1+z+2y}Mg_zAl_{11-z}O_{17+y} = \tfrac{1}{2}\cdot(Na_{1+z}Mg_zAl_{11-z}O_{17} + Na_{1+z+4y}Mg_zAl_{11-z}O_{17+2y}(O_{2y})_i). \qquad (12)$$

If $z = 1/3$ and $y = 1/6$, a composition results with 8.48% Na_2O; 2.21%MgO; balance Al_2O_3, which is not so far from the experimental composition of sample 1. The small differences can easily be accounted for by the presence of the 10% β-Al_2O_3 content. With regard to samples 2 and 3, a composition of $x = 0$ and $y \neq 0$ is practically identical to a composition of $x \neq 0$ and $y = 0$ as long as $3x = 2y$. Samples 1 to 3 can be used therefore to compare the models of Formulae 11 and 12. Samples 4 and 5 are limiting cases for both models, since $x = y = 0$ in these cases.

The first summand between the parentheses of Formula 12 is a fully magnesium stabilized ternary component phase. The second summand is a partially magnesium stabilized ternary component phase with oxygen interstitials in the conduction slab for additional charge compensation of the excess sodium ions. Contrary to the former model of Formula 11, the two component phases in Formula 12 do not differ in their spinel blocks, but in their conduction slabs. Therefore, the spinel block-determined values of the lattice constants a_0 of the two component phases of a sample must be identical, whereas the conduction slab-influenced lattice constants c_0 must be different. Consequently, all purely a_0-related $hk0$ diffraction lines cannot be significantly broadened, all hkl diffraction lines must be more or less split. The higher

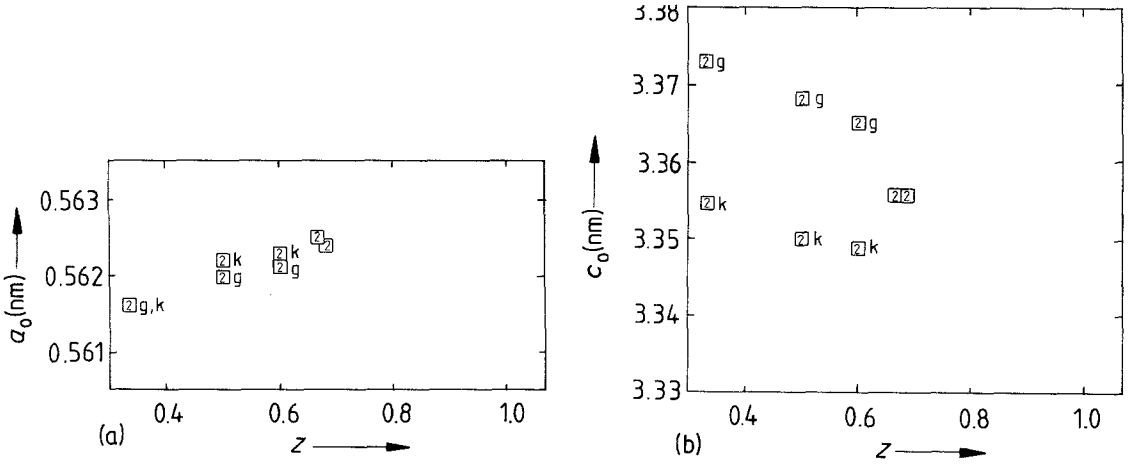

Figure 6 Dependence of the lattice constants (a) a_0 and (b) c_0 on the magnesium content z for ceramics with different compositions $Na_{1+3z+2y}Mg_zAl_{11-z}O_{17+y}$, but identical sodium contents $Na_{1\frac{2}{3}}$. For ceramics showing split diffraction lines, the lattice constants for both component phases g and k are given.

the $l^2/(h^2 + hk + k^2)$-ratio, the more they must be split. This has in fact been found experimentally. The new model withstood the test better than the model of Formula 11 and charge compensation by aluminium vacancies is discarded for β''-Al_2O_3 as it has already been done for β-Al_2O_3.

The lattice constants a_0 and c_0 of the component phases of samples 1 to 3 have been calculated by first associating left hand side, low angle and right hand side, high angle component lines of split peaks to a "g"- and a "k"-component phase, respectively, excluding broadened peaks from the calculation and associating all other peaks with no visible splitting to both component phases. The results are included in Table I and are additionally displayed in Figs. 6a and b.

The a_0-values for the two component phases of a sample are practically equal. They increase from sample 1 to samples 4/5, i.e. with increasing magnesium content as has already been discussed in Sections 4 and 5.

The c_0-values of the component phases of each of the samples 1 to 3, however, differ significantly. In addition, the c_0-values of either the g- or the k-component phases decrease from sample 1 to sample 3. The latter behaviour resembles the composition dependence of fully stabilized β''-Al_2O_3 discussed in Section 5, i.e. the lattice constant c_0 decreases with increasing sodium content, at least down to a certain level, which corresponds to $z = 0.8$.

Inspection of Formula 12 shows that the sodium content in fact increases with increasing magnesium content z for both component phases of each of the samples 1 to 3. This might be surprising on first sight, since samples 1 to 3 are stated as having nearly identical sodium contents. The contradiction that appears here can be resolved as follows.

Formula 12 is based on a one to one correspondence of fully and partially stabilized unit cells. Consequently, equal diffracted intensities for the component phases of samples 1 to 3 should result. This is true for sample 1 (see Fig. 2). An increase of z for the low sodium fully stabilized component phase as well as for the sodium rich partially stabilized component phase can now be balanced by a decrease of the number of unit cells of the sodium rich partially stabilized component phase without affecting the overall sodium content. An equivalent reduction in the intensities of the high angle component peaks of samples 2 and 3 supports this assumption. Furthermore, this is the first evidence that the high angle component peaks of split peaks have to be attributed to the partially stabilized β''-Al_2O_3 component phases, in other words that the partially stabilized component phases have to be associated with the k-component phases in Fig. 6. It follows that the g-component phases are to be associated with the fully stabilized component phases.

In Section 5, the height H of the conduction slab has been introduced. The z-dependence of H can now be used to support the above association of the two component phases of samples 1 to 3 with the two summands of Formula 12. H clearly decreases with increasing sodium content up to sodium contents corresponding to $z = 0.8$ inde-

pendent of any variation of a_0. This decrease has been attributed in Section 5 to an increasing polarization of the negatively charged spacer oxygen towards the adjacent positive sodium ions, as the content of positive sodium ions in the conduction slab increases.

Additional introduction of sodium ions into the conduction slab together with half as many charge compensating oxygen ions does not lead to a further increase of the positive charge content of the conduction slab. Yet, the ratio of positive to negative charges increases with the equivalent consequence that H decreases below the value that corresponds to the fully magnesium stabilized composition with the same magnesium content following from the same arguments used in Section 5.

This is the second argument that favours the identification of the k-component phases with the partially stabilized phases and of the g-component phases with the fully stabilized component phases.

The reduction of H cannot go further than to the limiting value 0.247 nm reached with $z = 0.8$ for fully stabilized compositions according to the same arguments given in Section 5.

The variation of H calculated for all component phases of the five samples of Table I is displayed in Fig. 7. The approximate agreement of the H_k-value of sample 1 on the one hand and of the H-values of the fully stabilized samples 4 (and 5) on the other hand or the even closer agreement of the right hand side, high-angle component peaks of the split reflections of sample 1 with the corresponding peaks of samples 4 (and 5) and the equivalently close agreement of the corresponding c_0-values must be regarded as accidental. The H- (and the c_0-) values of fully stabilized samples 4 and 5 must be seen rather as extensions of the H- (and c_0-) values of the H_g-component phases of samples 1 to 3.

This result is further corroborated by the z-dependences of the H-values of the g-component phases of samples 2 and 3. They fit into the respective places of the z-dependences of the H-values of fully magnesium stabilized β''-Al_2O_3 ceramics displayed in Fig. 5. Sample 1 is a special case, as it contains about 10% β-Al_2O_3 besides the required β''-Al_2O_3 phases and the extent of magnesium doping of the different phases therefore, is not known.

7. Conclusions

1. Fully stabilized ternary β''-Al_2O_3 ceramics with compositions corresponding to the Bettman–Peters formula $Na_{1+z}Mg_zAl_{11-z}O_{17}$ show the following dependences of the unit cell sizes upon sodium and magnesium contents. The lattice constant a_0 increases with increasing magnesium con-

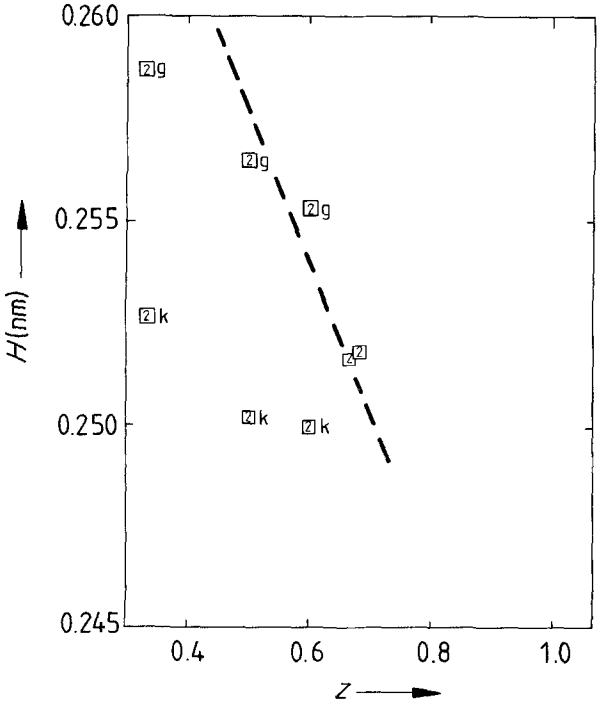

Figure 7 Dependence of the height H of the conduction slab on the magnesium content z for ceramics with different compositions $Na_{1+3z+2y}Mg_zAl_{11-z}O_{17+y}$, but identical sodium contents $Na_{1\frac{2}{3}}$. For ceramics showing split diffraction lines, the values for both component phases g and k are given. The z-dependence of H for fully magnesium stabilized β''-Al_2O_3 ceramics (Fig. 5) has been included for better reference (dashed line).

tent. In spite of a severe scatter in the data, an equational dependence may be stated as

$$a_0(z)/\text{nm} = 0.5595 + 0.00406z$$

at least for $0.5 \leqslant z < 0.8$. The lattice constant c_0 contains a contribution from a_0. It is therefore more appropriate to discuss the compositional dependence of the height H of the conduction slab. It decreases significantly with increasing sodium content as

$$H(z)/\text{nm} = 0.2761 - 0.03697z$$

over the range, $0.5 \leqslant z < 0.8$.

2. High resolution X-ray powder diffraction of magnesium stabilized β''-Al_2O_3 ceramics can resolve H_g, H_k-splittings of reflections indexed with a relatively high Miller index l, if the overall composition of a β''-Al_2O_3 ceramic sample does not correspond to the above formula. These splittings are connected with the simultaneous presence of two component β''-Al_2O_3 phases.

The two component phases do not differ in magnesium content i.e. in spinel block compositions but rather in sodium content, i.e. in the compositions of the conduction slabs. The H_g-component phase is attributed to the low-angle component peaks of the split diffraction lines and this component phase has the greater height of the conduction slab. It is fully magnesium stabilized in conformity with the Bettman–Peters formula. The H_k-component phase is attributed to the high-angle component peaks of the split diffraction lines. This component phase has the lower height of the conduction slab. It contains more sodium than the H_g-component phase but the same amount of magnesium. Therefore, it is only partially magnesium stabilized and the additional excess sodium ions are charge balanced by oxygen interstitials in the conduction slab. This compensation method corresponds to the Roth model for the charge compensation of excess sodium in β-Al_2O_3. The charge compensation mechanism based on aluminium vacancies is discarded for β''-Al_2O_3 as it has already been done for β-Al_2O_3.

Acknowledgements

This work is published by permission of Brown, Boveri and Cie Aktiengesellschaft. Support was received from the Bundesministerium für Forschung und Technologie under contract No. ET-4496 A. Thanks are due to L. Ziegelmüller for the preparation of the ceramic samples and to D. Stenzel and Dr J. Demny for recording the X-ray diffraction spectra and for fruitful discussions.

Appendix: Model calculation of the height of the conduction slab of β''-Al_2O_3 from the lattice constants a_0 and c_0

β''-Al_2O_3 is built up from an alternating sequence of spinel-like blocks and conduction slabs (Fig. A1). Each spinel block contains four layers of close-packed oxygen ions in cubic stacking extending normally to the c-axis. In contrast to β-Al_2O_3, the face-centred cubic packing of the oxygen ions of β''-Al_2O_3 is not confined to the spinel blocks, but also includes the spacer oxygen ions of the adjacent conduction slabs. The possible sites for oxygen ions in the conduction slabs are not fully occupied, and the spacer oxygen can therefore be regarded as the remainder of an oxygen layer in a cubic face-centred sequence.

Let us take a closer look at a single spinel block. Distortions of the close packing that are due to the insertion of aluminium or magnesium

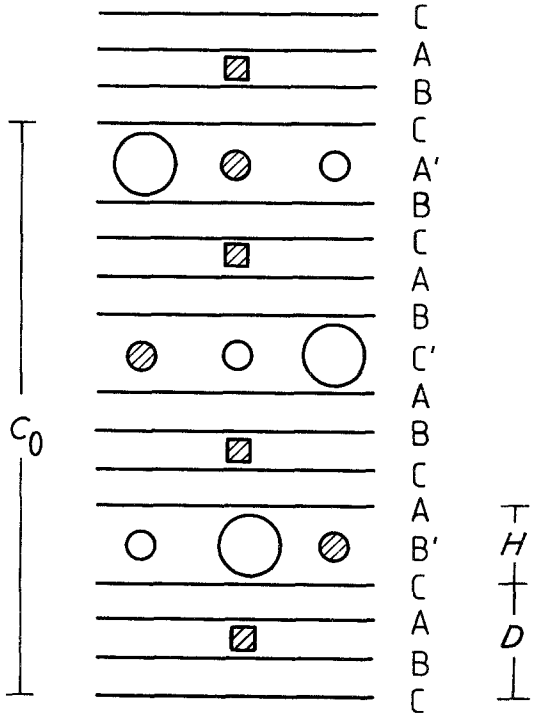

Figure A1 Schematic structure of non-stoichiometric fully magnesium stabilized β''-Al_2O_3. A hatched square stands for Al(2) aluminium sites in the centre of a spinel block with a z against $1-z$ fractional occupancy by magnesium and aluminium ions, respectively. Hatched small circles stand for a fractional presence of z "excess" sodium ions. The c-axis is defined by the layering direction and the a–b plane is perpendicular to it.

ions are neglected. Therefore the height of a fourfold oxygen layering is $D' = 4 \times 1.633 r_0$. If the extension of a spinel block is calculated in such a way that it corresponds to Fig. A1, i.e. with two spinel blocks separated by a whole spacer oxygen, then the overlapping of the two outermost oxygen layers with the respective spacer oxygens must be subtracted from D' to give

$$D = (3.266 - 0.1835)2r_0 = 3.0825 \times 2r_0. \quad \text{(A1)}$$

On the other hand, $2r_0 = a_0/2$ (see, for example, Fig. 3 of [6]). This relation inserted into Equation A1 yields

$$D = 1.5413 a_0. \quad \text{(A2)}$$

Finally, it has to be taken into account that one spinel block plus one spacer oxygen are only a third of the height c_0 of the hexagonal cell. The twisting of successive spinel blocks due to the rhombohedral screw axis will certainly not influence the extension of a single spinel block. Thus, the height H of the conduction slab, more correctly the diameter of the spacer oxygen in the direction of the c-axis, is

$$H = \frac{c_0}{3} - D = \frac{c_0}{3} - 1.5413 a_0. \quad (3)$$

References

1. G. YAMAGUCHI and K. SUZUKI, *Bull. Chem. Soc. Jpn.* **41** (1968) 93.
2. M. BETTMAN and C. R. PETERS, *J. Phys. Chem.* **73** (1969) 1774.
3. J. T. KUMMER, *Progr. Solid State Chem.* 7 (1972) 141.
4. J. FELSCHE, Jahresbericht 1976 an das BMFT; Projekt-Nr. ET4069: Entwicklung von Natrium/Schwefel-Akkumulatoren, Untersuchung des Feststoffelektrolyten β-Al_2O_3.
5. J. B. BATES, H. ENGSTROM, J. C. WANG, B. C. LARSON, N. J. DUDNEY and W. E. BRUNDAGE, *Solid State Ionics* 5 (1981) 159.
6. R. M. DELL and P. T. MOSELEY, *J. Power Sources* 6 (1981) 143.
7. J. P. BOILOT, G. COLLIN, PH. COLOMBAN and R. COMES, *Phys. Rev. B* **22** (1980) 5912.
8. G. J. MAY and C. M. B. HENDERSON, *J. Mater. Sci.* **14** (1979) 1229.
9. J. P. BOILOT, PH. COLOMBAN, G. COLLIN and R. COMES, *J. Phys. Chem. Solids* **41** (1980) 47.
10. J. P. BOILOT, PH. COLOMBAN, R. COLLONGUES, G. COLLIN and R. COMES, *ibid.* **41** (1980) 253.
11. C. A. BEEVERS and M. A. S. ROSS, *Z. Krist.* **97** (1937) 59.
12. J. FELSCHE, Jahresbericht 1978 an das BMFT: Entwicklung der Natrium/Schwefel-Batterie, Teilprojekt ET4176 A: Untersuchung des Feststoffelektrolyten β-Al_2O_3.
13. W. L. ROTH, *Trans. Amer. Crystallogr. Assoc.* **11** (1975) 51.
14. W. L. ROTH, F. REIDINGER and S. LA PLACA, in "Superionic Conductors", edited by G. D. Mahan and W. L. Roth (Plenum Press, New York, London, 1976) pp. 223–41.
15. W. HAYES, L. HOLDEN and B. C. TOFIELD, *Solid State Ionics* **1** (1980) 373.
16. A. K. RAY and E. C. SUBBARAO, *Mater. Res. Bull.* **10** (1975) 585.
17. F. HARBACH, "Sinterung von Festelektrolytkeramiken unter Einsatz von stöchiometrischer magnesium-stabilisierter Beta"-Tonerde", Proceedings of the 4th International Joint Meeting on Electro- and Magneto-ceramics, Celle, Germany, October 1981 (Deutsche Keramische Gesellschaft, Bad Honnef, 1982) pp. 128–41.
18. C. R. PETERS, M. BETTMAN, J. W. MOORE and M. D. GLICK, *Acta Crystallogr. B* **27** (1971) 1826.
19. J. L. BRIANT and G. C. FARRINGTON, *J. Solid State Chem.* **33** (1980) 385.
20. J. B. BATES, G. M. BROWN, T. DANEDA, W. E. BRUNDAGE, J. C. WANG and H. ENGSTROM in "Fast Ion Transport in Solids – Electrodes and Electrolytes", edited by P. Vashishta, J. N. Mundy and G. K. Shenoy (North-Holland, New York, Amsterdam, Oxford, 1979) pp. 261–66.
21. G. M. BROWN, D. A. SCHWINN, J. B. BATES and W. E. BRUNDAGE, *Solid State Ionics* **5** (1981) 147.
22. G. COLLIN, PH. COLOMBAN, J. P. BOILOT and R. COMES, in "Fast Ion Transport in Solids – Electrodes and Electrolytes", edited by P. Vashishta, J. N. Mundy and G. K. Shenoy (North-Holland, New York, Amsterdam, Oxford, 1979) pp. 312–14.
23. F. HARBACH, to be published.
24. D. SCHWARZENBACH, ETH Zürich: LATCON – a general program for the LS-refinement of lattice constants; this program has kindly been made available by Professor Felsche, University of Konstanz.
25. W. L. ROTH, General Electric Corporate Research and Development Report 74 CRD 054.
26. L. PAULING, "Die Natur der Chemischen Bindung" (Verlag Chemie, Weinheim, 1962).
27. J. C. WANG, *J. Chem. Phys.* **73** (1980) 5786.

Received 8th October 1982
and accepted 17 January 1983